

Exclusive processes in position space and the pion distribution amplitude

V. M. Braun

*Institut für Theoretische Physik, Universität Regensburg,
D-93040 Regensburg, Germany*

D. Müller

*Institut für Theoretische Physik II,
Ruhr-Universität Bochum,
D-44780 Bochum, Germany*

We suggest to carry out lattice calculations of current correlators in position space, sandwiched between the vacuum and a hadron state (e.g. pion), in order to access hadronic light-cone distribution amplitudes (DAs). In this way the renormalization problem for composite lattice operators is avoided altogether, and the connection to the DA is done using perturbation theory in the continuum. As an example, the correlation function of two electromagnetic currents is calculated to the next-to-next-to-leading order accuracy in perturbation theory and including the twist-4 corrections. We argue that this strategy is fully competitive with direct lattice measurements of the moments of the DA, defined as matrix elements of local operators, and offers new insight in the space-time picture of hard exclusive reactions.

PACS numbers: 12.38.-t, 14.20.Dh; 13.40.Gp

I. INTRODUCTION

Hadron light-cone distribution amplitudes (DAs) present the principal nonperturbative input in the pQCD description of hard exclusive reactions and are to a large extent complementary to the usual parton distributions. The existing information on DAs is, however, very limited. The main reason for this is that the DAs are much more difficult to access experimentally: for realistic momentum transfers, the contributions of interest are often contaminated by large nonperturbative corrections coming from the end-point regions in the quark momentum fraction.

The pion leading twist DA is the simplest one and has attracted most attention. There is increasing evidence that at the scale of the order of 1 GeV this DA differs considerably from its asymptotic form. In particular, QCD sum rule estimates [1, 2], lattice calculations [3] and the analysis of the experimental data on the transition form factor $\gamma^* \rightarrow \pi\gamma$ [1, 4, 5] are consistent with the positive value of the second Gegenbauer moment of the pion DA which is roughly a factor two below the original estimate by Chernyak and Zhitnitsky [6]. Beyond the second moment, very little is known. The analysis of the $\gamma^* \rightarrow \pi\gamma$ form factor in Ref. [1, 4] indicates a negative value for the fourth Gegenbauer moment, but the status of this result is not clear as the analysis

has some model dependence. The lattice calculations of the fourth and higher Gegenbauer moments would be very difficult because they contribute with a small coefficient, and because the lattice renormalization of local operators with many derivatives becomes too cumbersome. The aim of this letter is to suggest an alternative approach, based on the lattice calculation of exclusive amplitudes in coordinate space. We will argue that the interpretation of such calculations in the framework of QCD factorization is equally straightforward and offers new insights compared to the standard momentum space formulation. From the lattice side, the advantage is that the renormalization problem for composite operators is avoided altogether, but, instead, in order to be sensitive to the detailed structure of the pion DA, one needs pion sources with large momentum, at least of order 2–3 GeV.

The idea to emphasize the coordinate rather than momentum-space dependence of the correlation functions is by itself not new, see e.g. [7, 8]. Our proposal goes in the same direction as the work [9, 10], the difference is that we suggest to calculate physical observables that are free from renormalization uncertainties. Also, we demonstrate that the analysis of such correlation functions in continuum theory is aided by the conformal operator product expansion.

The presentation is organized in follows. In Sec. II

we introduce the coordinate-space correlation function of two electromagnetic currents sandwiched between vacuum and the pion. We calculate this correlation function to leading order (LO) in QCD perturbation theory and discuss the physical interpretation. In Sec. III the state-of-the-art (next-to-next-to-leading order) calculation of this correlation function is presented, including two-loop radiative corrections and nonperturbative twist-4 effects. The main result of this analysis is that the QCD corrections remain well under control for all pion momenta. In Sec. IV we discuss possible strategies and the potential accuracy of the extraction of the pion distribution amplitude from the coordinate space dependence of this correlation function, assuming that it is measured in a limited range of distances accessible in lattice calculations. The corresponding setup and several possible generalizations are discussed in Sec. V, which also contains a summary and our final conclusions.

II. EXAMPLE

As an example, we consider the correlation function of two electromagnetic currents sandwiched between vacuum and the pion state

$$T_{\mu\nu} = \langle 0 | T \{ j_\mu(x) j_\nu(-x) \} \pi^0(p) \rangle, \quad (2.1)$$

where

$$j_\mu(x) = \frac{2}{3} \bar{u}(x) \gamma_\mu u(x) - \frac{1}{3} \bar{d}(x) \gamma_\mu d(x), \quad (2.2)$$

which is the coordinate space analog of the pion transition form factor involving two photons. Note that one and the same correlation function (2.1) enters the pion decay $\pi^0 \rightarrow \gamma\gamma$ and the form factors $\gamma^* \rightarrow \pi^0\gamma^*$ for two virtual or $\gamma^* \rightarrow \pi^0\gamma$ for one virtual and one real photons. Differences arise at the stage when one goes over to the states with given momenta: depending on the virtuality, different coordinate space regions are emphasized/suppressed by the Fourier transform.

At small space-like separations $|x^2| \ll 1/\Lambda_{\text{QCD}}^2$ the amplitude in (2.1) can be calculated using the operator product expansion (OPE). To LO in the strong coupling, the answer is obtained from the diagram in Fig. 1 and reads:

$$T_{\mu\nu} = -\frac{5i}{9} f_\pi \epsilon_{\mu\nu\rho\sigma} \frac{x^\rho p^\sigma}{8\pi^2 x^4} T(p \cdot x, x^2) \quad (2.3)$$

with

$$T(p \cdot x, x^2) = \int_0^1 du e^{i(2u-1)p \cdot x} \phi_\pi(u, \mu). \quad (2.4)$$

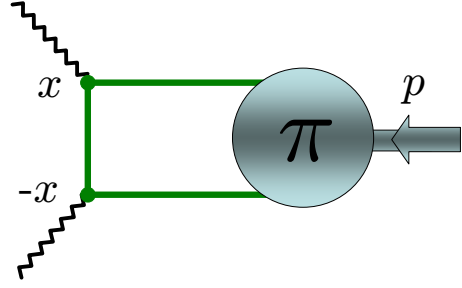


FIG. 1: Leading-order contribution to the correlation function (2.1)

The relevant nonperturbative input is provided by the pion DA defined as

$$\begin{aligned} \langle 0 | \bar{q}(a_1 n) \gamma_\mu \gamma_5 q(a_2 n) \pi^0(p) \rangle &= \\ &= i f_\pi p_\mu \int_0^1 du e^{-ipn(\bar{u}a_1 + ua_2)} \phi_\pi(u, \mu), \end{aligned} \quad (2.5)$$

where $f_\pi = 93$ MeV is the pion decay constant, $\bar{u} \equiv 1 - u$, n_μ is a light-light vector, $n^2 = 0$, and μ is the normalization scale, which is set to be of the order $1/\sqrt{|x^2|}$.

In the following we write the pion DA as an expansion over Gegenbauer polynomials,

$$\phi_\pi(u, \mu) = 6u\bar{u} \sum_{n=0}^{\infty} \phi_n(\mu) C_n^{3/2}(2u-1), \quad (2.6)$$

and use the fact that the Fourier transform

$$\begin{aligned} 8 \int_0^1 du u\bar{u} e^{i\rho(2u-1)} C_n^{3/2}(2u-1) &= \\ &= \sqrt{2\pi} (n+1)(n+2) i^n \rho^{-3/2} J_{n+3/2}(\rho) \end{aligned} \quad (2.7)$$

leads to Bessel functions. To our accuracy we obtain then for the correlation function (2.4)

$$T(p \cdot x, x^2) = \frac{3}{4} \sum_{n=0}^{\infty} \phi_n(\mu) \mathcal{F}_n(p \cdot x) \quad (2.8)$$

with

$$\mathcal{F}_n(\rho) = i^n \sqrt{2\pi} \frac{(n+1)(n+2)}{2} \rho^{-3/2} J_{n+3/2}(\rho). \quad (2.9)$$

We will view this result (2.8) as a partial wave expansion of the correlation function $T(\rho = p \cdot x, x^2)$. (a group theoretical explanation will be given below). The partial waves $\mathcal{F}_n(\rho)$, expressed by Bessel functions $J_{n+3/2}(\rho)$ with half integer index, are simply given in terms of trigonometric functions, e.g.,

we have for $n = 0$: $\mathcal{F}_0(\rho) = 2[\sin(\rho) - \rho \cos(\rho)]/\rho^3$. In particular this term, appearing as the leading one in the expansion (2.8), corresponds to the contribution of the asymptotic distribution amplitude, while $\mathcal{F}_2(\rho)$ and $\mathcal{F}_4(\rho)$ take into account contributions of the second, $C_2^{3/2}(2u - 1)$, and the fourth, $C_4^{3/2}(2u - 1)$, Gegenbauer moments, respectively. Note that only even values of n contribute to the series because of C -parity conservation. The used approximation allows for a partonic interpretation of the correlation function $T(p \cdot x, x^2)$, which is obvious: it corresponds to a probability amplitude of the valence quark distribution in the pion in the longitudinal distance (“Ioffe-time”) $\rho = p \cdot x$ at transverse distance x^2 .

The partial waves $\mathcal{F}_0(\rho)$, $-\mathcal{F}_2(\rho)$ and $\mathcal{F}_4(\rho)$ are plotted in Fig. 2. These oscillating functions are

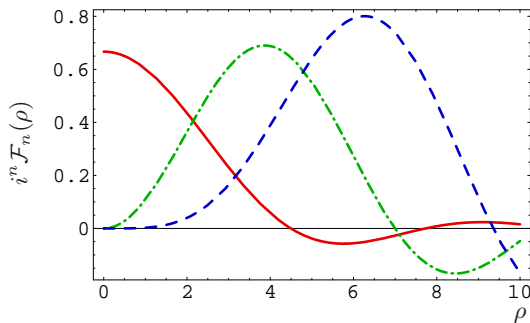


FIG. 2: From left to right: $\mathcal{F}_0(\rho)$ (solid), $-\mathcal{F}_2(\rho)$ (dash-dotted), $\mathcal{F}_4(\rho)$ (dashed).

strongly peaked at a position that moves with increasing index n to the r.h.s. and so the contribution of the asymptotic DA and the corrections are well separated. On the other hand, large values of $p \cdot x$ and, hence, of the pion momentum are needed to probe higher-order Gegenbauer moments efficiently.

To see this, we plot in Fig. 3 the correlation function $T(\rho, x^2)$, given in the approximation (2.8), as a function of $\rho = p \cdot x$ for the asymptotic pion DA (dashed curve), and for the model with $\phi_2 = 0.25$ and two choices $\phi_4 = 0.1$ and $\phi_4 = -0.1$, respectively, cf. Fig. 4.

Note that the value of $T(\rho, x^2)$ at $\rho = 0$ is equal to $1/2$ in our normalization (up to radiative and higher twist corrections discussed in the next Section) and does not depend on the shape of the pion DA. The deviation from the asymptotic DA (dashed curve) for a realistic model is significant starting $\rho \sim 1$. The dependence on ϕ_4 , taken as $\phi_4 = 0.1$ (dash-dotted curve) and $\phi_4 = -0.1$ (solid curve), becomes visible at distances $\rho \geq 3 - 4$. We remark that a more closer look, given in Sect. IV, reveals that a partial wave analysis might allow to access the forth

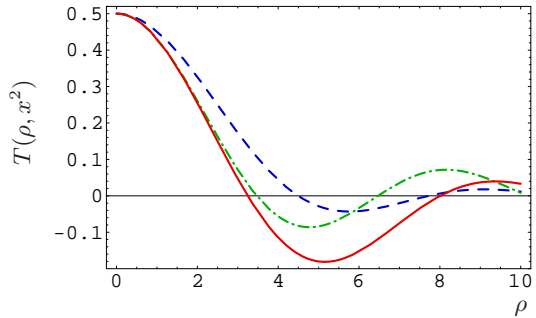


FIG. 3: The correlation function $T(\rho, x^2)$, leading-order (2.8), calculated using asymptotic pion DA (dashed), the model with $\phi_2 = 0.25$ and two choices $\phi_4 = 0.1$ (dash-dotted) and $\phi_4 = -0.1$ (solid).

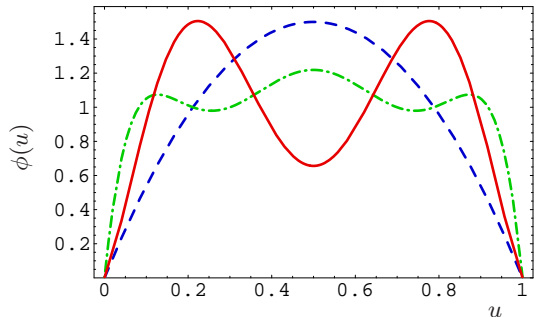


FIG. 4: Models for the pion DA as specified in Fig. 3.

Gegenbauer moment even for $\rho \lesssim 3$. With increasing ρ the correlation function changes sign and becomes negative, unless the fourth Gegenbauer moment is larger as the second one, which seems to be unlikely (not shown).

The ρ -behavior of the models, plotted in Fig. 3, results from the cos-Fourier transform (2.4) of the DA (because for a symmetric DA the sin-component dies out) and can qualitatively be understood as follows. The position of the first zero at $\rho = \rho_0$ gives us the effective width π/ρ_0 of the DA in momentum space. For instance, a flat DA $\phi_\pi(u) = 1$ corresponds to $\rho_0 = \pi$, an equal momentum sharing DA $\phi_\pi(u) = \delta(u - 1/2)$ leads to a constant correlation function, i.e., $\rho_0 \rightarrow \infty$, while the effective width of the asymptotic DA follows from $\rho_0 \approx 1.43\pi$. Compared to the asymptotic DA, for the realistic models, shown by the solid and the dash-dotted curves, the first zero is shifted to the left, which indicates that these DAs are broader than the asymptotic one, cf. Fig. 4. The difference between the solid and the dash-dotted models, on the other hand, is mostly pronounced near the first minimum. The magnitude of the correlation function at this minimum $\rho = \rho_1$ is a measure for the overlap of the DA with

the harmonic $\cos((2u-1)\rho_1)$ which is maximized at $u_1 = 1/2 - \pi/\rho_1 \sim 0.2$. It is large for the models with a two-hump DA like the one of Ref. [1], where it was also argued that all higher Gegenbauer moments are negligible. It is much smaller for a dash-dotted model corresponding to a flat (albeit still oscillating) DA as shown in Fig. 4. These oscillations are not significant and can be understood as an artifact of truncating the conformal spin partial wave expansion. In fact, a conjectured ADS/QCD model $\phi^{\text{ADS/QCD}} = (8/\pi)\sqrt{u(1-u)}$ [11, 12] gives rise to a similar shape. We add to our discussion that very narrow DA's and those with nodes, leading to huge resonance effects, are clearly distinguishable in the correlation function from those shown in Fig. 3, even at smaller values of ρ .

III. STATE-OF-THE-ART

The previous discussion was mainly qualitative. In this section we present the state-of-the-art calculation of the correlation function $T(p \cdot x, x^2)$, defined in Eq. (2.3), in next-to-next-to-leading (NNLO) of perturbative QCD and including the twist-four corrections.

An adequate technical framework is provided by the conformal operator product expansion (OPE). Recall that the expansion in Gegenbauer polynomials in (2.6) alias the partial wave decomposition in (2.8) to LO are governed by conformal symmetry: the expansion is organized as the irreducible decomposition of the product of two currents into conformal operators. The partial waves specified in Eq. (2.9) are nothing but the LO Wilson-coefficients of the leading twist operators in the conformal OPE. They can be viewed as the Clebsch–Gordon coefficients of the collinear conformal group $SL(2, \mathbb{R})$ and are labelled by the conformal spin $j = n + 2$, for a review see Ref. [14]. The advantage of such a decomposition is that the Gegenbauer moments do not mix under evolution in LO or, in other words, the conformal spin is a good quantum number to this accuracy.

Taking into account radiative corrections to the leading twist Wilson-coefficients translates to the modification of the partial waves which become scale- (and scheme-) dependent:

$$\mathcal{F}_n(\rho) \rightarrow \mathcal{F}_n(\rho, -\mu^2 x^2; \alpha_s(\mu)).$$

In turn, the higher-twist corrections yield x^2 suppressed additive terms and for our present purposes it is convenient to reexpand them in terms of the leading-twist partial waves taken to leading-order.

We end up with the expansion of the form

$$\begin{aligned} T(\rho, x^2) &= \\ &= \frac{3}{4} \sum_{n=0}^{\infty} \phi_n(\mu^2) \mathcal{F}_n(\rho, -\mu^2 x^2; \alpha_s(\mu)) + O(\alpha_s^3) \\ &\quad + \frac{3}{4} x^2 \sum_{n=0}^{\infty} \phi_n^{(4)}(\mu^2) \mathcal{F}_n(\rho) + O(x^2 \alpha_s) + O(x^4), \end{aligned} \quad (3.10)$$

where $\phi_n^{(4)}$ are related to the matrix elements of twist-four operators, weighted with specific Wilson coefficients. Viewed this way, both the corrections to the partial waves and the twist-4 coefficients $\phi_n^{(4)}(\mu^2)$ are specific for the considered correlation function. The Gegenbauer moments $\phi_n(\mu^2)$ are universal, however, they depend on the scheme conventions.

In what follows we consider separately perturbative and twist-four corrections in some detail.

A. Perturbative corrections

The next-to-leading (NLO) perturbative corrections to the pion transition form factor were calculated in the minimal subtraction ($\overline{\text{MS}}$) scheme in Refs. [15–17] and were supplemented by the evaluation of the logarithmical scale change [18–21]. In addition NNLO diagrams that are proportional to n_f , the number of light quark flavors, have been evaluated in the same scheme [22]. This result can be used to obtain the NNLO corrections that are proportional to $\beta_0 = (11/3)C_A - (2/3)n_f$, the first coefficient appearing in the QCD beta-function $\beta(g)/g = -(\alpha_s/4\pi^2)\beta_0 + O(\alpha_s^2)$. Finally, the constraints imposed by the conformal symmetry, tested at NLO level [23, 24], have been used to obtain the missing terms at NNLO. A detailed NNLO analysis can be found in Ref. [26], see also Appendix A for a discussion of different factorization schemes. A Fourier transform of these results provides one with the radiative corrections to the correlation function (2.3) in position space.

It is instructive to consider the results in the hypothetical conformal limit, in which the β function is vanishing (which means, technically, that the β_0 proportional terms are omitted). In this case the modification of the partial waves, cf. Eq. (3.10), is entirely governed by conformal symmetry:

$$\begin{aligned} \mathcal{F}_n &= C_n(\alpha_s) (-\mu^2 x^2)^{\frac{\gamma_n}{2}} i^n \sqrt{\pi} \frac{(n+1)(n+2)}{4} \\ &\quad \times \frac{\Gamma(n+5/2 + \gamma_n/2)}{\Gamma(n+5/2)} \left(\frac{\rho}{2}\right)^{-\frac{3+\gamma_n}{2}} J_{n+\frac{3+\gamma_n}{2}}(\rho). \end{aligned} \quad (3.11)$$

As compared to the LO expressions (2.9), the ρ dependence is modified by the anomalous dimensions $\gamma_n(\alpha_s)$, which alter, e.g., the index of Bessel functions. In addition the normalization is changed by the factor

$$C_n(\alpha_s) = \frac{\Gamma(2 - \gamma_n/2)\Gamma(1 + n)}{\Gamma(1 + n + \gamma_n/2)} c_n(\alpha_s), \quad (3.12)$$

where $c_n(\alpha_s)$ are the Wilson coefficients that appear in polarized deep inelastic scattering structure function g_1 and are known to NNLO [27]. Since of conformal symmetry, a scale change does not lead to a mixing of conformal partial waves (3.12) or the Gegenbauer moments.

One possibility to go beyond the conformal limit is to restore both the scale dependence of the coupling and the renormalization logs within the normalization condition of Ref. [26]. This scheme is discussed in Appendix A; we refer to it as the conformal subtraction scheme, the $\overline{\text{CS}}$ scheme. We will use the renormalization group improved partial waves, defined in Eq. (A.11), for the numerical analysis. In general, the anomalous dimensions govern the evolution of the Gegenbauer moments with respect to a scale change:

$$\mu \frac{d}{d\mu} \phi_n(\mu^2) = -\gamma_n(\alpha_s(\mu)) \phi_n(\mu^2) + \dots \quad (3.13)$$

Even in the $\overline{\text{CS}}$ scheme which is designed to make maximal use of the conformal symmetry, we expect that the Gegenbauer moments will mix under evolution, indicated by the ellipsis. This mixing is induced by the trace anomaly and gives rise to a $(\alpha_s/2\pi)^2 \beta_0 \ln(-x^2 \mu_0^2)$ proportional contribution which, however, vanishes at a reference scale $-x^2 = 1/\mu_0^2$. We expect that this unknown NNLO mixing effect is small and can safely be ignored.

The partial waves in the conventional $\overline{\text{MS}}$ scheme can be obtained from those in $\overline{\text{CS}}$ by the appropriate transformation. In particular the Gegenbauer moments in these two schemes are related as

$$\phi_n^{\overline{\text{CS}}} = \phi_n^{\overline{\text{MS}}} - \frac{\alpha_s}{2\pi} \sum_{m=0}^{n-2} B_{nm}^{(1)} \phi_m^{\overline{\text{MS}}} + O(\alpha_s^2). \quad (3.14)$$

The matrix $B_{nm}^{(1)}$ is known explicitly and is given in Eq. (A.16) of Appendix A. This relation is also valid in the hypothetical conformal limit. Note that the $\overline{\text{MS}}$ Gegenbauer moments are given by a finite sum of those in the $\overline{\text{CS}}$. Consequently, plugging Eq. (3.14) into Eq. (3.10), one sees that in the $\overline{\text{MS}}$ scheme all conformal partial waves (3.11) are excited even if a truncated model for the DA is used. We stress that the scheme independence of the correlation function

is only guaranteed if the Gegenbauer moments are rotated at the given input scale. Taking the same model in different schemes will in general lead to different predictions for the correlation function.

As we will see in Sect. IV, such scheme-dependent mixing effects are numerically important. For illustration, consider the asymptotic DA which we define here as the zero mode of the evolution kernel in a given scheme and order of perturbation theory. By construction, the asymptotic DA does not evolve under scale transformations. In the $\overline{\text{CS}}$ scheme to NLO this amounts to the same choice of the Gegenbauer coefficients as in LO: $\phi_0 = 1$ and $\phi_n = 0$ for $n > 0$. The one-loop corrections to the correlation function (3.10) are then given by

$$T^{\text{as}} \simeq \frac{3}{4} \left[1 - \frac{\alpha_s(\mu)}{\pi} + \mathcal{O}(\alpha_s^2) \right] \mathcal{F}_0(\rho). \quad (3.15)$$

The current conservation implies $\gamma_0(\alpha_s) = 0$, protecting the ρ -dependence of the lowest partial wave from radiative corrections. In the $\overline{\text{MS}}$ scheme, on the other hand, the Gegenbauer moments of the asymptotic DA for $n \geq 2$ are nonzero and are obtained by the rotation (3.14):

$$\begin{aligned} \phi_n^{\text{as}-\overline{\text{MS}}} &= \frac{\alpha_s(\mu)}{2\pi} \frac{8C_F(2n+3)}{n(n+1)(n+2)(n+3)} \\ &\times \left(S_1(n+2) - \frac{n+3}{2(n+1)} \right) + \mathcal{O}(\alpha_s^2), \end{aligned} \quad (3.16)$$

whereas the normalization, i.e., $\phi_0 = 1$, remains unchanged. The excitation of higher Gegenbauer moments is, however, rapidly decreasing with n : For $n = \{2, 4, 6, 8\}$ we find the values $\{0.124, 0.039, 0.018, 0.009\}$ in units of $\alpha_s(\mu)$, respectively. A more extensive discussion about scheme dependence can be found in Ref. [29].

Finally, the limit $\rho \rightarrow 0$ of the correlation function (2.3) yields the analog of the Bjorken sum rule in polarized deep inelastic scattering:

$$T(\rho = 0, x^2) \simeq \frac{1}{2} C_0(-\mu^2 x^2, \alpha_s(\mu)). \quad (3.17)$$

In this limit, which is independent on the factorization scheme, any information contained in the DA is washed out. Hence, this sum rule is a *pure* QCD prediction, which is known as perturbative expansion to three loop order [28].

After these general remarks, we consider the perturbative corrections for the particular models of the pion DA specified in Sect. II. We assume that the models are defined at the scale 1 GeV and set the factorization scale to $\mu^2 = -1/x^2$. For the demonstration we consider two current separations: a larger

one $-x^2 = 1/\text{GeV}^2$ [$\approx (0.2 \text{ fm})^2$] and a smaller one $-x^2 = 1/4\text{GeV}^2$ [$\approx (0.1 \text{ fm})^2$]. In the latter case evolution of Gegenbauer moments is taken into account: The leading logs are resummed and non-leading ones are consistently combined with the $\alpha_s/2\pi$ power expansion of the correlation function (3.10), for details see, e.g., Ref. [26]. The coupling is specified at the normalization point $\mu = 2 \text{ GeV}$ to be $\alpha_s = 0.36$ and $\alpha_s = 0.3$ at LO and NLO, respectively.

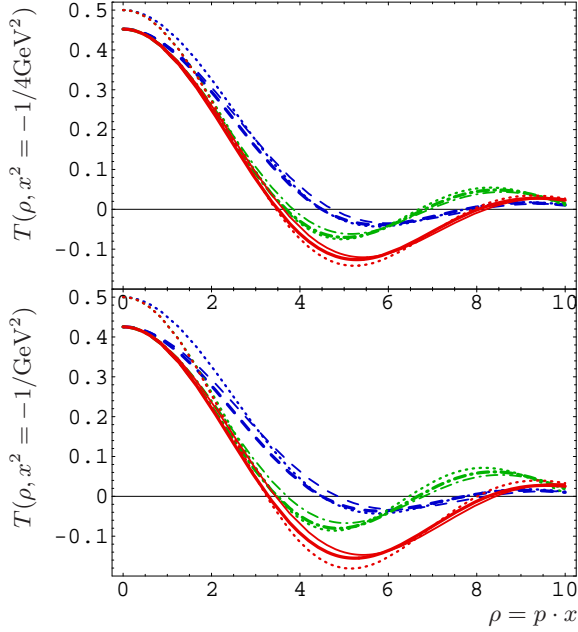


FIG. 5: NLO predictions for the correlation function (2.3) in the $\overline{\text{MS}}$ scheme (thin) and rotated to the $\overline{\text{CS}}$ one (thick) at the scale $-x^2 = 1/\text{GeV}^2$ (lower panel) $-x^2 = 1/4\text{GeV}^2$ (upper panel) compared to the LO results (dots) for the three models of the pion DA shown in Fig. 4.

The NLO results are shown in Fig. 5 for $-x^2 = 1/\text{GeV}^2$ and $-x^2 = 1/4\text{GeV}^2$ in the lower and upper panel, respectively. Notice that the perturbative corrections lead to a universal shift of the value at $\rho = 0$, which is $1/2$ in LO, downwards to $1/2(1 - \alpha_s/\pi)$ which is about -15% for the larger and -9% for the smaller separation between the currents, respectively. This effect is entirely due to the negative NLO correction in the sum rule (3.17).

Besides the overall normalization, perturbative corrections result in a slight change of the ρ dependence, seen as a shift of zeros and extrema to larger ρ values (compare thin and dotted lines). This scheme dependent effect arises from the excitation of higher conformal partial waves, as discussed above, and is more pronounced at larger separations (lower panel). Note that the ρ -dependence corresponding to the

asymptotic DA (dashed curves), evaluated in the $\overline{\text{CS}}$ scheme (thick curves), is not affected, see Eq. (3.15). For the other two models in the $\overline{\text{CS}}$ scheme only a slight shift of extrema appears, which is visible in the lower panel at larger values of ρ (compare thick and dotted lines). A more quantitative look reveals that in general the absolute size of radiative correction grows somewhat with increasing ρ .

Note that at smaller distances the model dependence slightly weakens, compare the magnitude of solid or dash-dotted curves at the first minima in the upper and lower panel. This is caused by evolution, which does not change the value at $\rho = 0$, however, reduces Gegenbauer moments with a strength that grows with increasing conformal spin. Obviously, even at $-x^2 = 1/4\text{GeV}^2$ the model predictions remain clearly distinguishable.

The NNLO corrections evaluated in the $\overline{\text{CS}}$ scheme (not shown) lead to a further decrease of the normalization, so that the net reduction for $\rho = 0$ is, compared to LO, -25% and -13% for $-x^2 = 1/\text{GeV}^2$ and $-x^2 = 1/4\text{GeV}^2$, respectively. The modification of the ρ dependence is, however, negligible as compared to the NLO result in the $\overline{\text{CS}}$ scheme, and is hardly visible even for the larger separation $-x^2 = 1/\text{GeV}^2$. As mentioned above, mixing effects due to the NNLO evolution are not taken into account, but are expected to be tiny.

B. Higher-twist Corrections

Higher-twist corrections are in general suppressed by full powers of the separation x^2 between the currents. In particular, including twist-four contributions one obtains

$$T(p \cdot x, x^2) = \int_0^1 du e^{i(2u-1)p \cdot x} t(u, x^2), \quad (3.18)$$

where

$$t(u, x^2) = \phi_\pi(u) + \frac{x^2}{4} \phi_4(u) - x^2 \int_0^u d\alpha_1 \int_0^{\bar{u}} d\alpha_2 \\ \times \left[\frac{1}{\alpha_3} \tilde{\Phi}_4(\underline{\alpha}) + \frac{(u - \bar{u} - \alpha_1 + \alpha_2)}{\alpha_3^2} \Phi_4(\underline{\alpha}) \right]. \quad (3.19)$$

The leading-twist perturbative corrections are not shown for brevity. The notations correspond to Ref. [30], where one can find the definitions and the corresponding expressions for the twist-four distribution amplitudes to the next-to-leading conformal spin accuracy. In the last term α_1, α_2 and $\alpha_3 = 1 - \alpha_1 - \alpha_2$ are the quark, antiquark and gluon

momentum fractions, respectively. Including the contributions of the lowest and the next-to-lowest conformal spin one obtains [30, 31]

$$\begin{aligned}\phi_4(u) &= \frac{200}{3} \delta_\pi^2 u^2 \bar{u}^2 + 21 \delta_\pi^2 \omega_{4\pi} \left\{ u\bar{u}(2 + 13u\bar{u}) \right. \\ &\quad \left. + [2u^3(6u^2 - 15u + 10) \ln u] + [u \leftrightarrow \bar{u}] \right\}, \\ \tilde{\Phi}_4(\underline{\alpha}) &= 120 \alpha_1 \alpha_2 \alpha_3 \delta_\pi^2 \left[-\frac{1}{3} + \frac{21}{8} \omega_{4\pi} (3\alpha_3 - 1) \right], \\ \Phi_4(\underline{\alpha}) &= 120 \alpha_1 \alpha_2 \alpha_3 (\alpha_1 - \alpha_2) \delta_\pi^2 \frac{21}{8} \omega_{4\pi}.\end{aligned}\quad (3.20)$$

The nonperturbative parameters δ_π^2 and $\omega_{4\pi}$ are defined as reduced matrix elements of local operators, for example

$$\langle 0 | \bar{q} i g \tilde{G}_{\mu\nu} \gamma_\nu q | \pi^0(p) \rangle = -f_\pi \delta_\pi^2 p_\mu. \quad (3.21)$$

Numerical estimates for these matrix elements are available from QCD sum rules:

$$\delta_\pi^2 = (0.18 \pm 0.06) \text{ GeV}^2, \quad \omega_{4\pi} = 0.2 \pm 0.1 \quad (3.22)$$

at the scale 1 GeV [$\delta_\pi^2 = (0.14 \pm 0.05) \text{ GeV}^2$, $\omega_{4\pi} = 0.13 \pm 0.07$ at the scale 2 GeV], see Ref. [30] and the references therein.

Note that beyond the leading conformal spin accuracy the twist-four contributions are not polynomials [31]. Plugging Eq. (3.20) into Eq. (3.19), we find, however, that the next-to-leading conformal spin contributions completely cancel each other and the leading conformal spin yields the total $O(x^2)$ correction:

$$t(u, x^2) = \phi_2(u) + x^2 \frac{8}{9} \delta_\pi^2 \cdot 30u^2 \bar{u}^2. \quad (3.23)$$

This can be effectively rewritten as the correction to the first two leading twist Gegenbauer coefficients $1 \rightarrow 1 + (8/9)x^2 \delta_\pi^2$, $\phi_2 \rightarrow \phi_2 - (8/9)(1/6)x^2 \delta_\pi^2$. Hence, we have

$$\phi_0^{(4)}(\mu) = \frac{8}{9} \delta_\pi^2(\mu), \quad \phi_2^{(4)}(\mu) = -\frac{8}{54} \delta_\pi^2(\mu). \quad (3.24)$$

The upper bound for the contributions to (3.20) of higher conformal spins can be obtained using the renormalon model of Ref. [37]. These extra contributions mainly influence the large ρ -behavior of the correlation function while the numbers in (3.24) are not affected. We see that, to LO accuracy, higher-twist correction produce an additive shift in the physical values of the Gegenbauer moments of the pion DA, which is calculable, at least in principle.

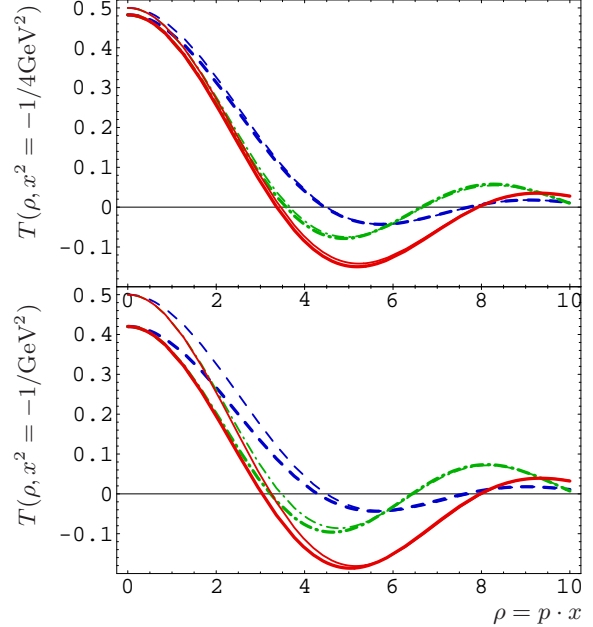


FIG. 6: LO predictions for the correlation function (2.3) with (thick) and without (thin curves) twist-four corrections for two choices of the quark-interquark separation: $-x^2 = 1/\text{GeV}^2$ (lower panel) and $-x^2 = 1/4 \text{ GeV}^2$ (upper panel). Models for pion DA are the same as used for the LO predictions, shown by dotted curves, in Fig. 3.

Beyond LO, one may define effective partial waves,

$$\mathcal{F}_n^{\text{eff}}(\rho, x^2) = \mathcal{F}_n(\rho, -x^2 \mu^2; \alpha_s(\mu)) + x^2 \frac{\phi_n^{(4)}(\mu)}{\phi_n(\mu)} \mathcal{F}_n(\rho), \quad (3.25)$$

that additively combine perturbative and higher twist corrections together. Here, the evolution of the twist-four coefficient is governed by the difference in the LO anomalous dimensions of the corresponding operators:

$$\frac{\phi_n^{(4)}(\mu)}{\phi_n(\mu)} = \left(\frac{\alpha_s(\mu)}{\alpha_s(\mu_0)} \right)^{\frac{32/9 - \gamma_n^{(0)}}{\beta_0}} \frac{\phi_n^{(4)}(\mu_0)}{\phi_n(\mu_0)}, \quad (3.26)$$

where $\gamma_0^{(0)} = 0$ and $\gamma_2^{(0)} = 50/9$. Note that these effective partial waves depend on the non-perturbative quantities, which induces some model dependence.

As it is demonstrated in Fig. 6, twist-four contributions are significant at $-x^2 = 1/\text{GeV}^2$ (lower panel) and much less important at $-x^2 = 1/4 \text{ GeV}^2$ (upper panel). In particular, for $-x^2 = 1/\text{GeV}^2$ the value at $\rho = 0$ decreases by about 16% which is comparable to the NLO perturbative correction, whereas for $-x^2 = 1/4 \text{ GeV}^2$ the decrease is only by $\sim 3.5\%$ which is roughly one third of the respective NLO effect. Note that the ρ dependence of separate

partial waves is not affected by the twist-four contributions. Their magnitude is changing, however: the second partial wave is enhanced and the lowest one somewhat suppressed by the twist-four corrections. These effects depend linearly on x^2 and are additionally suppressed by evolution.

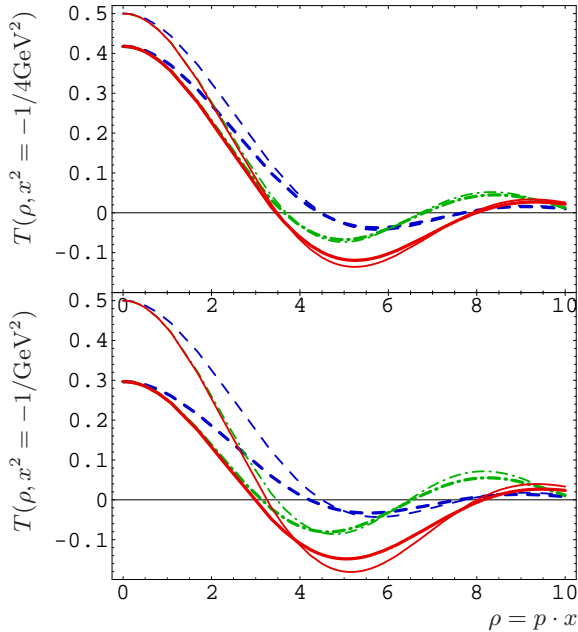


FIG. 7: Combined NNLO and twist-four predictions for the correlation function (2.3) in the $\overline{\text{CS}}$ scheme (thick curves) compared to the LO results (thin curves). The factorization scale is set to the quark-interquark separation, $\mu^2 = -1/x^2$, which is $-x^2 = 1/\text{GeV}^2$ ($-x^2 = 1/4 \text{GeV}^2$) for the lower (upper) panel, respectively. Models for pion DA are the same as in Fig. 3.

Our final predictions combining the perturbative effects to NNLO accuracy in the $\overline{\text{CS}}$ scheme and the twist-four corrections are shown by thick curves in Fig. 7 and compared to the corresponding leading-order leading twist predictions (thin curves). For the separation $-x^2 = 1/4 \text{GeV}^2$ the overall correction is rather small. The normalization at $\rho = 0$ is reduced by about 17%, whereas the zeros and positions of extrema are essentially fixed. We remind that there will be small flow of these points in the $\overline{\text{MS}}$ scheme, cf. upper panel in Fig. 5. The overall corrections for $-x^2 = 1/\text{GeV}^2$ are much larger.

The conclusion is that the correlation function (2.3) can be calculated in QCD to a high accuracy. In particular for $-x^2 \lesssim 1/4 \text{GeV}^2 \sim (0.1 \text{ fm}^2)$ the perturbation theory works rather well and the higher-twist effects do not exceed 3%.

The next question to address is whether the knowledge of the correlation function (2.3) can be used to constrain the shape of the pion DA and, for

example, allow for an accurate determination of the few lowest Gegenbauer moments.

IV. REVEALING THE PION DA

Let us first consider the QCD prediction for the normalization of the correlation function in the vicinity of $\rho = 0$. Here only the lowest partial wave contributes, while higher ones are suppressed as

$$|\mathcal{F}_n(\rho)| \leq \frac{(n+1)(n+2)\sqrt{\pi}}{4\Gamma(n+5/2)} \left| \frac{\rho}{2} \right|^n. \quad (4.27)$$

Note the factorial suppression factor. For the favored value of $\phi_2 \sim 0.25$, we find for $\rho \simeq 1/4 [\simeq 1/2]$ that the contamination of the second partial wave is already below three per mil [about 1%], respectively. All higher partial waves can certainly be omitted. We remind that a strong suppression of higher partial waves occurs also in momentum space, if both photons have a large virtuality [25, 26]. It follows that to three per mil [1%] accuracy the sum rule (3.17) can be extended for $\rho \leq 1/4[1/2]$:

$$T(\rho \sim 0, x^2) = \left[C_0(1, \alpha_s(-1/x^2)) + \frac{8}{9} x^2 \delta_\pi^2 \right] \frac{3}{4} \mathcal{F}_0(\rho) + O(\alpha_s x^2) + O(x^4), \quad (4.28)$$

where $(3/4)\mathcal{F}_0(\rho) = 1/2 - \rho^2/20 + O(\rho^4)$. We emphasize again that in the $\overline{\text{CS}}$ scheme the radiative corrections to the lowest partial wave are absent at the normalization point. We expect that the excitation of higher partial waves due to the evolution yields a negligible $O(\rho^2 \alpha_s^2)$ effect, see also Eq. (3.14) and the discussion of the $\overline{\text{MS}}$ mixing. Hence, in this scheme, the perturbative corrections can be borrowed from the Bjorken sum rule, known to order α_s^3 [28]. For shortness we display the two-loop result:

$$C_0^{(2)}(-\mu^2 x^2, \alpha_s(\mu)) = 1 - \frac{\alpha_s(\mu)}{\pi} - \frac{\alpha_s^2(\mu)}{\pi^2} \times \left(\frac{55 - 4n_f}{12} + \frac{\beta_0}{4} \ln(-x^2 \mu^2 e^{2\gamma_E - 1}) \right). \quad (4.29)$$

Note that due to the Fourier transform the argument of the renormalization logs is decorated with a transcendent number $e^{2\gamma_E - 1} \approx 1.166994 \dots$.

To predict the normalization of the correlation function, we have to specify the QCD coupling. The world average value of α_s , given at the Z -boson mass scale, reads to three loop accuracy [32]

$$\alpha_s^{(3)}(\mu = 91.18 \text{ GeV}) = 0.1184 \pm 0.003. \quad (4.30)$$

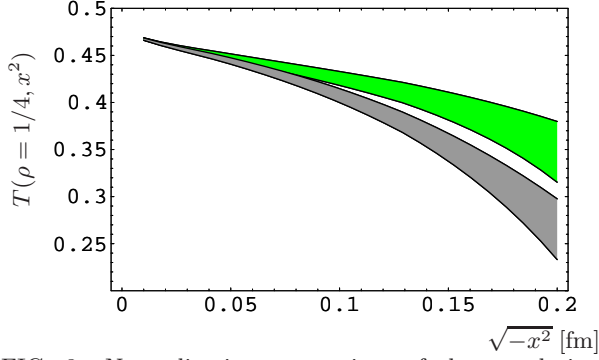


FIG. 8: Normalization uncertainty of the correlation function (2.3) for $\rho = 1/4$. The upper error band entirely arises by the uncertainty of the running coupling, while the lower one takes also into account twist-four contamination within the central value, given in Eq. (3.22).

In the backward evolution to a lower scale we take into account quark thresholds, treated in the standard way [33]. For $\rho = 0$ and the current separation $-x^2 = 1/4\text{GeV}^2 \sim (0.1\text{ fm})^2$ we obtain, including three-loop and higher-twist effects::

$$T(0, -1/4\text{GeV}^2) = 0.430_{-0.007}^{+0.008} - 0.018_{-0.006}^{+0.006}, \quad (4.31)$$

where the number of quarks is set to $n_f = 4$. The predicted twist-four correction is comparable to the error induced by the uncertainty of α_s , see Fig. 8, where the dependence of $T(0, x^2)$, including the error bands, is displayed as a function of x^2 .

Next we discuss the access to the Gegenbauer moments. We assume that the correlation function is measured in a certain interval of pion momenta alias an interval in ρ , $\rho_0 \leq \rho \leq \rho_{\text{max}}$. Since an overall normalization might be difficult, we consider the ratio

$$R(\rho_0, \rho, x^2) = \frac{T(\rho, x^2)}{T(\rho_0, x^2)}, \quad \rho_0 < \rho, \quad (4.32)$$

which is normalized to one at $\rho = \rho_0$. Requiring that $\rho_0 < 1$ allows to truncate the partial wave expansion in the denominator at the second term $\sim \phi_2$. As the result, $R(\rho_0, \rho, x^2)$ is essentially a linear function of ϕ_n with $n > 2$.

The maximal accessible value of ρ , given by ρ_{max} , is limited by the pion momentum that is feasible in a lattice calculation. We assume here that $\rho_{\text{max}} < 3$, i.e., lower than the first zero of the lowest conformal partial wave, cf. Fig. 2. Staying away from the zero allows one to consider the subtracted ratio to access directly the second Gegenbauer moment:

$$\mathcal{M}(\rho_0, \rho, x^2) = 1 - \frac{R(\rho_0, \rho, x^2)}{\mathcal{R}_0(\rho_0, \rho)}, \quad \rho_0 < \rho \lesssim 3, \quad (4.33)$$

where $\mathcal{R}_n(\rho_0, \rho) = \mathcal{F}_n(\rho)/\mathcal{F}_0(\rho_0)$. Since $\mathcal{R}_0(\rho_0, \rho)$ only decreases by at most a factor three in the whole range $\rho \lesssim 3$, this weight does not introduce any numerical instability. The conformal spin expansion of \mathcal{M} in terms of ratios of the effective partial waves (3.25) reads:

$$\mathcal{M}^{(4)} \simeq \frac{[\mathcal{R}_2^{\text{eff}}(\rho_0) - \mathcal{R}_2^{\text{eff}}(\rho)] \phi_2}{1 + \mathcal{R}_2^{\text{eff}}(\rho_0) \phi_2} - \frac{\mathcal{R}_4^{\text{eff}}(\rho) \phi_4}{1 + \mathcal{R}_2^{\text{eff}}(\rho_0) \phi_2}, \quad (4.34)$$

where

$$\mathcal{R}_n^{\text{eff}}(\rho, x^2) = \frac{\mathcal{F}_n^{\text{eff}}(\rho, x^2)}{\mathcal{F}_0^{\text{eff}}(\rho, x^2)}. \quad (4.35)$$

Here we neglected all contributions in ϕ_6, ϕ_8 , etc. from the expansion in the numerator. The corresponding truncation error is estimated to be on the per mil [percentage] level for $\rho < 2$ [3], respectively. For example, for $\rho = 3$ we find to LO accuracy:

$$\mathcal{M} - \mathcal{M}^{(4)} \sim 3 \cdot 10^{-4} \phi_4 + 7 \cdot 10^{-2} \phi_6 + 3 \cdot 10^{-3} \phi_8. \quad (4.36)$$

Here the first term on the r.h.s. comes from the truncation in the dominator (assuming $\rho_0 = 1/2$) and can safely be neglected, same as the contribution of ϕ_8 . The remaining term in ϕ_6 effectively induces a small additive uncertainty in determination of the first two Gegenbauer moments. For instance, assuming values of $\mathcal{M}^{(4)}$ are known for two different values $\rho = 2$ and $\rho = 3$, we find by solving the set of two linear equations:

$$\delta\phi_2 \approx -0.01\phi_6 \quad \delta\phi_4 \approx -0.13\phi_6. \quad (4.37)$$

Assuming $\phi_6 \sim 0.1$ the errors induced by the truncation of the partial wave expansion are in this version negligible for ϕ_2 and probably on the one percent level for ϕ_4 . We remind that convergency of the Gegenbauer expansion in the vicinity of $u = 0$ ($u = 1$), which is required if the DA vanishes at the end points, leads to an upper bound for the large- n behavior of the coefficients $|\phi_n| < \text{const}/n^p$ with $p > 1$, so that large values of ϕ_n with $n > 4$ are increasingly unlikely. Clearly, a fitting procedure including ϕ_6 is also possible. This is demonstrated in Fig. 9, where the effect on \mathcal{M} is shown for the ϕ_6 varied in the interval $-0.2 \dots 0.2$, which we consider as an overestimation.

Radiative corrections to the ratio (4.32) of the correlation function are much milder as compared to their overall normalization. A precision analysis requires a careful specification of the running coupling. We take the world average value (4.30) and calculate the corresponding value at the scale $\mu = 2\text{ GeV}$ by the tree loop evolution equation within $n_f = 4$:

$$\alpha_s(\mu = 2\text{ GeV}) = 0.304_{-0.021}^{+0.024}. \quad (4.38)$$

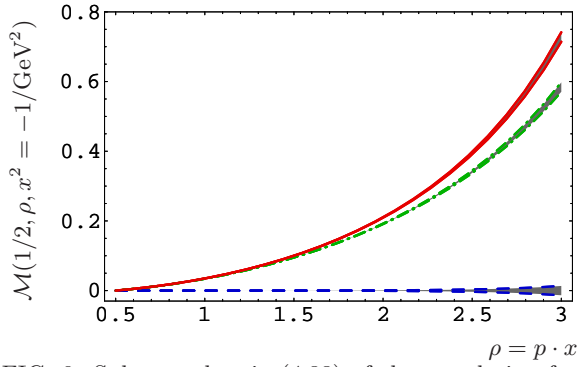


FIG. 9: Subtracted ratio (4.33) of the correlation function (2.3) calculated at LO as a function of ρ with $\rho_0 = 1/2$ and $-x^2 = 1/\text{GeV}^2$. Models of the pion DA are same as in Fig. 3, where the splitting of curves shows the possible (overestimated) contribution of higher conformal partial waves with $n > 4$.

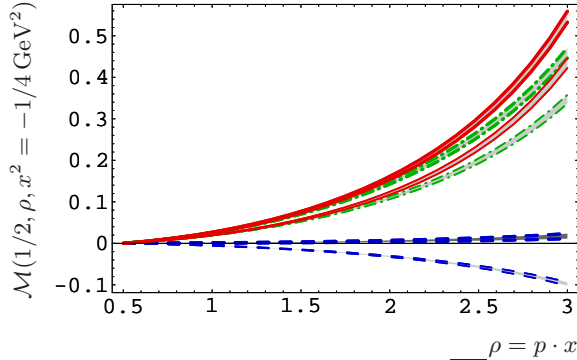


FIG. 10: Same as in Fig. 9 to NLO for the $\overline{\text{MS}}$ (thin) and $\overline{\text{CS}}$ radiative (thick) schemes. The variation within the predicted twist-four corrections are shown as error band. Here $-x^2 = 1/4 \text{ GeV}^2$ and the coupling is specified by the central values (4.38).

We note that the resulting central value and errors of α_s at two loop accuracy are compatible with the given one; it is, however, in the heart of perturbation theory that the specification of α_s to LO accuracy goes hand in hand with large uncertainties. As discussed in Sect. III A, the asymptotic DA at NLO in the $\overline{\text{MS}}$ differs from that in the $\overline{\text{CS}}$ scheme, mainly for the $n = 2$ and $n = 4$ moments, see Eq. (3.16). This effect is seen in Fig. 10, where the subtracted ratio \mathcal{M} (4.34) calculated in the $\overline{\text{MS}}$ scheme using the LO asymptotic DA (thin dashed curve) clearly deviates from zero. This deviation is removed for the corrected asymptotic DA (3.16), for which the $n = 2$ moment is ≈ 0.04 . For the same reason, the other two model predictions in the $\overline{\text{MS}}$ scheme (thin curves) are systematically shifted downwards compared to the $\overline{\text{CS}}$ (thick curves). A

small deviation from zero for the prediction corresponding to the asymptotic DA in the $\overline{\text{CS}}$ scheme (thick dashed curve) comes from the excitation of the $n = 2$ partial wave by a twist-four contribution. The shown narrow error bands arise from the variation of the twist-four parameter in the range $\delta_\pi^2(\mu = 2 \text{ GeV}^2) = 0.09 \dots 0.19 \text{ GeV}^2$.

Since perturbative corrections to the partial waves in the $\overline{\text{CS}}$ scheme only induce a small modification of the ρ dependence in the considered range (absent for the lowest one and on the one percent or lower level for higher ones), the extraction of the first few Gegenbauer moments can be considerably simplified. To this end, we define the effective Gegenbauer moments:

$$\Phi_n^{\text{eff}} = \frac{C_n(\langle\langle\rho\rangle\rangle_n|\alpha_s, -x^2\mu^2)\phi_n + x^2\phi_n^{(4)}}{C_0(\alpha_s, -x^2\mu^2) + (8/9)x^2\delta_\pi^2}, \quad (4.39)$$

which depend on the average value of ρ in the given range ($\langle\langle\rho\rangle\rangle_n \sim 2$ for $\rho_{\text{max}} \sim 3$).

The subtracted ratio (4.34) in the range $\rho_0 \leq \rho \leq \rho_{\text{max}}$ can be written to a good accuracy in terms of the effective moments as

$$\mathcal{M}^{(4)} \simeq \frac{[\mathcal{R}_2(\rho_0) - \mathcal{R}_2(\rho)]\Phi_2^{\text{eff}}}{1 + \mathcal{R}_2(\rho_0)\Phi_2^{\text{eff}}} - \frac{\mathcal{R}_4(\rho)\Phi_4^{\text{eff}}}{1 + \mathcal{R}_2(\rho_0)\Phi_2^{\text{eff}}}, \quad (4.40)$$

where $\mathcal{R}_n(\rho) = \mathcal{F}_n(\rho)/\mathcal{F}_0(\rho)$ is the ratio of the LO partial waves (2.9).

The relation between the effective moments and the physical Gegenbauer moments in the expansion of the pion DA includes radiative and higher twist corrections. As an illustration, for $\langle\langle\rho\rangle\rangle_n = 2.2$ and at $\mu = 2 \text{ GeV}$ we find

$$\begin{aligned} \phi_2(2 \text{ GeV}) &= [0.961_{-0.003}^{+0.003} - 0.03_{-0.01}^{+0.01}] \Phi_2^{\text{eff}} \\ &+ 0.005_{-0.002}^{+0.002} + \dots, \end{aligned} \quad (4.41)$$

$$\phi_4(2 \text{ GeV}) = [0.902_{-0.008}^{+0.008} - 0.03_{-0.01}^{+0.01}] \Phi_4^{\text{eff}} + \dots$$

The first term in the square brackets corresponds to the perturbative correction while the second one arises from the twist-four contribution. Note that the normalization change due to radiative corrections is only on the level of 4% for ϕ_2 and 10% for ϕ_4 , respectively, and is comparable with the higher twist correction. In NNLO we find a slight increase of the normalization $0.961 \rightarrow 0.982$ and $0.902 \rightarrow 0.951$ (for $n_f = 4$), whereas the error is drastically reduced. The residual factorization and the renormalization scale dependence also prove to be very small.

As the final step, the Gegenbauer moments in the $\overline{\text{MS}}$ scheme to NLO follow from

$$\phi_2^{\overline{\text{MS}}} = \phi_2 + \frac{7}{18} \frac{\alpha_s}{\pi} + O(\alpha_s^2), \quad (4.42)$$

$$\phi_4^{\overline{\text{MS}}} = \phi_4 + \frac{209}{810} \frac{\alpha_s}{\pi} \phi_2 + \frac{11}{90} \frac{\alpha_s}{\pi} + O(\alpha_s^2).$$

V. CONCLUSION

A typical setup for a lattice calculation of the correlation function (2.1) would be to take the separation between the two currents purely spacelike, $x^\mu \rightarrow \{0, \vec{x}\}$, and integrate over the c.m. position of the currents with a certain three-dimensional momentum. Since the pion coupling to the source is usually momentum dependent, the simplest strategy would probably be to consider ratios of the correlation function calculated for the same pion momentum but different \vec{x} (and different c.m. momenta of the pair of currents), thus creating the set of “data points” with correlated values of $x^2 = -|\vec{x}|^2$ and $\rho = \vec{p} \cdot \vec{x}$. In this way the dependence on the pion coupling cancels out. The crucial condition for such a calculation is to have a sufficient “lever arm” in ρ . For a lattice spacing a the momentum cannot be larger than

$$|\vec{p}| < a^{-1},$$

which translates to the restriction on the maximal accessible value of ρ

$$\rho_{\text{max}} < \frac{|\vec{x}|}{a}.$$

In other words, ρ cannot be larger than (half of) the separation between the currents in lattice units. Since, on the other hand, perturbative treatment of the correlation function is possible for $|\vec{x}| \leq 0.2$ fm, this requirement translates to a necessity to work on a fine lattice with $a < 0.03 - 0.05$ fm. This presents a considerable challenge for an unquenched calculation. The advantage of this formulation is, however, that the problem of (nonperturbative) renormalization of lattice operators is avoided altogether.

For a demonstration, we have chosen in this work to consider the correlation function of two electromagnetic current in which case the perturbative expansion is known to the NNLO accuracy. This choice may be inconvenient for a lattice calculation because of the epsilon-tensor appearing as a prefactor in (2.3). This problem can easily be avoided by

considering a correlation function of a vector and an axial-vector current, e.g.,

$$T'_{\mu\nu} = \langle 0 | T \{ \bar{q}(x) \gamma_\mu q(x) \bar{q}(-x) \gamma_\nu \gamma_5 q(-x) \} \pi^0(p) \rangle. \quad (5.43)$$

More importantly, the same strategy can be used to extract information about the B-meson distribution amplitude in the heavy quark limit from the lattice measurement of the correlation function of the type

$$\langle 0 | T \{ \bar{h}_v(x) \gamma_\mu q(x) \bar{q}(-x) \Gamma q(-x) \} | B_v(p) \rangle, \quad (5.44)$$

where v is the heavy quark velocity and h_v an effective heavy-quark field operator, which can be calculated in terms of the B-meson DA using soft-collinear effective theory [38–40]. The standard method (calculation of the moments) is not applicable in this case, since the existing definition of the B-meson DA relies entirely on a perturbative factorization; the relation with the Wilson operator expansion is lost unless an additional energy cutoff is introduced, see [41, 42].

Finally, nucleon distribution amplitudes [43, 44] can be studied in the same manner, from the correlation functions involving a local baryon current.

Acknowledgements

V.B. is grateful to IPPP for hospitality and financial support during his stay at Durham University where this work was finalized. This work has been partially supported by the Verbundforschung (Hadrons and Nuclei) of the German Federal Ministry for Education and Research (BMBF) (Contract 06 BO 103) and by the EU Integrated Infrastructure Initiative Hadron Physics Project under contract number RII3-CT-2004-506078.

APPENDIX A: PERTURBATIVE EXPANSION

The radiative corrections in the position space might be obtained from those in the momentum space by Fourier transform:

$$\frac{i\epsilon_{\mu\nu\rho\sigma} x^\rho p^\sigma}{8\pi^2 x^4} T(p \cdot x, x^2) = \int \frac{d^4 q}{(2\pi)^4} e^{2i q \cdot x} \frac{i\epsilon_{\mu\nu\rho\sigma} q^\rho p^\sigma}{q^2} \tilde{T}(\omega, -q^2), \quad (A.1)$$

where the hard scattering amplitude $\tilde{T}(\omega, -q^2)$ is expressed by the asymmetry variable $\omega = -q \cdot p/q^2$ and $q = (q_1 - q_2)/2$. Note that to LO accuracy the normalization is chosen to be $\tilde{T}(\omega = 0) = 1$. The correlation function is given by the partial wave expansion:

$$\tilde{T}(\omega, -q^2) = \sum_{\substack{n=0 \\ \text{even}}}^{\infty} \tilde{\mathcal{F}}_n(\omega, -\mu^2/q^2; \alpha_s(\mu)) \phi_n(\mu^2). \quad (\text{A.2})$$

In the hypothetical conformal limit the running coupling is replaced by its non-trivial fixed point value, at which the β -function vanishes. Then the predictive power of the conformal operator product expansion can be used to obtain the partial waves:

$$\tilde{\mathcal{F}}_n(\omega, -\mu^2/q^2 | \gamma_n) = c_n(\alpha_s) \frac{(n+1)(n+2)\sqrt{\pi}}{2^{n+2}\Gamma(n+5/2)} \left(\frac{\mu^2}{-q^2} \right)^\epsilon \omega^n {}_2F_1 \left(\begin{matrix} (n+1+\epsilon)/2, (n+2+\epsilon)/2 \\ (n+5+\epsilon)/2 \end{matrix} \middle| \omega^2 \right) \Big|_{\epsilon=\gamma_n/2}. \quad (\text{A.3})$$

Here

$$\gamma_n(\alpha_s) = \frac{\alpha_s}{2\pi} \gamma_n^{(0)} + \frac{\alpha_s^2}{(2\pi)^2} \gamma_n^{(1)} + O(\alpha_s^3), \quad \gamma_n^{(0)} = C_F \left(4S_1(n+1) - \frac{2}{(n+1)(n+2)} - 3 \right) \quad (\text{A.4})$$

are the anomalous dimensions and

$$c_n = 1 + \frac{\alpha_s}{2\pi} c_n^{(1)} + \dots, \quad c_n^{(1)} = C_F \left(S_1^2(n+1) - S_2(n+1) + \frac{3}{2} S_1(n+2) + \frac{3 - 2S_1(n)}{2(n+1)(n+2)} - \frac{9}{2} \right) \quad (\text{A.5})$$

are the Wilson coefficients, normalized to one ($c_n^{(0)} \equiv 1$) at LO, of the polarized deeply inelastic structure function g_1 for the flavor non-singlet sector. Both of them are evaluated in the momentum space within the $\overline{\text{MS}}$ scheme. The NLO anomalous dimensions can be found, e.g., in Ref. [34], and the few lowest one to NNLO in Ref. [35]. The NNLO expressions (or numerical values for the few lowest) Wilson-coefficients c_n are obtained from Ref. [36]. All numbers, used in this paper, are collected in Ref. [26].

To transform the conformal predictions (A.3) into the position space, we first utilize the standard integral representation for hypergeometric functions and in addition a quadratic transformation:

$${}_2F_1 \left(\begin{matrix} (n+1+\epsilon)/2, (n+2+\epsilon)/2 \\ (n+5+\epsilon)/2 \end{matrix} \middle| \omega^2 \right) = \frac{\Gamma(2n+4+2\epsilon)}{\Gamma(n+2+\epsilon)^2} \int_0^1 du \frac{[(1-u)u]^{n+1+\epsilon}}{(1+\omega-2\omega u)^{n+1+\epsilon}}. \quad (\text{A.6})$$

Plugging Eq. (A.3) into Eq. (A.2), and interchanging u and q integration in Eq. (A.1), the Fourier transform can now be easily performed by means of:

$$\int \frac{d^4 q}{(2\pi)^2} e^{2ix \cdot q} \left(\frac{\mu^2}{-q^2} \right)^\epsilon \frac{\bar{q}_\rho}{\bar{q}^2} \left(\frac{p \cdot \bar{q}}{-\bar{q}^2} \right)^n = \frac{1}{16\pi^2} \frac{\Gamma(2-\epsilon)}{\Gamma(1+n+\epsilon)} \frac{x_\rho (-x^2 \mu^2)^\epsilon}{(-x^2)^2} (-ip \cdot x)^n e^{i(2u-1)x \cdot p}, \quad (\text{A.7})$$

where $\bar{q} = q + (2u-1)p/2$. Here p^2 and p_ρ terms are neglected to leading twist accuracy (the latter drops out after contraction with the Levi-Civita tensor). Finally, the u -integration leads to the partial waves (3.11) in position space within the Wilson coefficients (3.12).

The conformal symmetry breaking due to the trace anomaly appears the first time as $\alpha_s^2 \beta_0$ correction. It contains the renormalization logs, needed to restore the renormalization group invariance in the perturbative expansion with respect to a running coupling $\alpha_s(\mu)$, and induces a mixing of Gegenbauer moments, which depends on the factorization scheme. It is purely conventional how we are dealing with this mixing. Appealing possibilities are

- i. combining the conformal predictions (A.3) with the diagrammatical $\overline{\text{MS}}$ result [22],
- ii. the partial waves matches at the normalization point $-q^2 = \mu^2$ the conformal predictions (A.3),
- iii. the Gegenbauer moments evolve autonomously.

Certainly, the latter case is the most appealing ones, however, it requires the full NNLO result for the trace anomaly induced term (in an arbitrary scheme). Unfortunately, the corresponding piece of the NNLO anomalous dimensions is unknown. Hence, we are only able to follow the first two suggestions, where the mixing due to evolution remains unknown [26]. It turned out that the numerical differences of the constant $\beta_0\alpha_s^2/2$ proportional terms of these both schemes, are moderate. Moreover, it is expected that the mixing effect due to the evolution is tiny. We remind that in the $\overline{\text{MS}}$ scheme such a mixing under evolution already appears at NLO and leads in fact only to small numerical effects.

Following the second suggestion, we present here the NNLO corrections in the so-called $\overline{\text{CS}}$ scheme. To do so we restore in the conformal predictions (A.3) the scale dependence of the coupling, i.e., $\alpha_s \rightarrow \alpha_s(\mu)$, and the renormalization logs, which are governed by the renormalization group equation

$$\left[\mu \frac{\partial}{\partial \mu} + \beta(\alpha_s) \frac{\partial}{\partial g} \right] \tilde{\mathcal{F}}_n(\omega, -\mu^2/q^2; \alpha_s(\mu)) = \gamma_n(\alpha_s(\mu)) \tilde{\mathcal{F}}_n(\omega, -\mu^2/q^2; \alpha_s(\mu)) + O(\alpha_s^3), \quad (\text{A.8})$$

approximated to NNLO. The remaining freedom is fixed by the requirement that at the normalization point $-q^2 = \mu^2$ the partial waves coincide with those in Eq. (A.3). A more detailed discussion is given in Ref. [26]. The so found result,

$$\tilde{\mathcal{F}}_n(\omega, -\mu^2/q^2; \alpha_s(\mu)) = \tilde{\mathcal{F}}_n(\omega, -\mu^2/q^2 | \gamma_n(\alpha_s(\mu))) - \frac{\beta_0 \alpha_s^2(\mu)}{2 (2\pi)^2} \Delta_n^{(2,\beta)}(\omega, -\mu^2/q^2) + O(\alpha_s^3), \quad (\text{A.9})$$

is understood as a perturbative expansion up to NNLO accuracy, where the addenda,

$$\Delta_n^{(2,\beta)}(\omega, -\mu^2/q^2) = \ln(-\mu^2/q^2) \frac{\partial}{\partial(\alpha_s/2\pi)} \left(1 + \frac{1}{2} \gamma_n(\alpha_s) \ln(-\mu^2/q^2) \right) \tilde{\mathcal{F}}_n(\omega, -\mu^2/q^2 | \gamma_n(\alpha_s)) \Big|_{\alpha_s=0} \quad (\text{A.10})$$

restores the renormalization group invariance.

Again utilizing Eq. (A.7) as expansion with respect to ϵ , the Fourier transform of the addenda (A.10) is straightforward. Combining the resulting expression with the perturbative expansion of the conformal predictions (3.11) and (3.12) we find up to order α_s^2 :

$$\mathcal{F}_n(\rho, -x^2\mu^2; \alpha_s(\mu)) = \left[1 + \frac{\alpha_s(\mu)}{2\pi} C_n^{(1)}(\rho, -x^2\mu^2) + \frac{\alpha_s^2(\mu)}{(2\pi)^2} C_n^{(2)}(\rho, -x^2\mu^2) + O(\alpha_s^3) \right] \mathcal{F}_n(\rho), \quad (\text{A.11})$$

where $\mathcal{F}_n(\rho)$ is the LO partial wave (2.9) and

$$C_n^{(1)} = c_n^{(1)} + \frac{s_n^{(1)}(\rho, -x^2\mu^2)}{2} \gamma_n^{(0)}, \quad C_n^{(2)} = c_n^{(2)} + \frac{s_n^{(1)}}{2} \left(\gamma_n^{(1)} + c_n^{(1)} \gamma_n^{(0)} \right) + \frac{s_n^{(2)}}{8} \left(\gamma_n^{(0)} \right)^2 - \frac{\beta_0}{2} C_n^{(2,\beta)}. \quad (\text{A.12})$$

The ‘shift’ functions

$$s_n^{(m)}(\rho, -x^2\mu^2) = \frac{d^m}{d\epsilon^m} (-\mu^2 x^2)^\epsilon \frac{\Gamma(2-\epsilon)\Gamma(1+n)}{\Gamma(1+n+\epsilon)} \frac{\mathcal{F}_n(\rho, -x^2\mu^2 | 2\epsilon)}{\mathcal{F}_n(\rho)} \Big|_{\epsilon=0} \quad (\text{A.13})$$

depend on the variables $-x^2\mu^2$ and ρ . To obtain the renormalization group improved Wilson-coefficients we restore the scale dependence of the coupling, i.e., $\alpha_s \rightarrow \alpha_s(\mu)$, and take into account

$$C_n^{(2,\beta)} = \left[\left(\frac{\gamma_n^{(0)}}{4} \text{Ln}_n(-x^2\mu^2) - C_n^{(1)}(\rho, -x^2\mu^2) \right) \text{Ln}_n(-x^2\mu^2) + \frac{3}{4} \gamma_n^{(0)} (1 - S_2(n)) \right], \quad (\text{A.14})$$

where $\text{Ln}_n(-x^2\mu^2) = \ln(-x^2\mu^2) - S_1(n) + 2\gamma_E - 1$. We finally remark that the following substitutions restores the result in momentum space:

$$\mathcal{F}_n(\rho) \Rightarrow \tilde{\mathcal{F}}_n(\omega) = \frac{(n+1)(n+2)\sqrt{\pi}}{2^{n+2}\Gamma(n+5/2)} \omega^{n+2} F_1 \left(\begin{matrix} (n+1)/2, (n+2)/2 \\ (n+5)/2 \end{matrix} \middle| \omega^2 \right),$$

$$s_n^{(m)}(\rho, -x^2\mu^2) \Rightarrow s_n^{(m)}(\omega, -\mu^2/q^2) = \frac{d^m}{d\epsilon^m} \left(\frac{\mu^2}{-q^2} \right)^\epsilon \frac{{}_2F_1\left(\frac{(n+2\epsilon+1)/2, (n+2\epsilon+2)/2}{n+2\epsilon+5/2} \middle| \omega^2\right)}{{}_2F_1\left(\frac{(n+1)/2, (n+2)/2}{n+5/2} \middle| \omega^2\right)} \Bigg|_{\epsilon=0}, \quad (\text{A.15})$$

$$C_n^{(2,\beta)}(\rho, -\mu^2x^2) \Rightarrow C_n^{(2,\beta)}(\omega, -\mu^2/q^2) = \left(C_n^{(1)}(\omega, -\mu^2/q^2) + \frac{1}{2}\gamma_n^{(0)} \ln(-\mu^2/q^2) \right) \ln(-\mu^2/q^2).$$

The NLO corrections to the correlation function in the $\overline{\text{MS}}$ scheme might be obtained by Fourier transform from the known result in momentum space [15–17]. Representing the hard-scattering part as a convolution of the LO hard-scattering part within some kernels, see Ref. [23], the transformation can be straightforwardly performed by utilizing Eq. (A.7) for $n = 0$. Alternatively, we can simply rotate the partial waves (A.11) in the $\overline{\text{CS}}$ scheme, expanded up to NLO. Note that the trace anomaly does not enter in this approximation. The non-vanishing entries of the rotation matrix, used in Eq. (3.14),

$$B_{nm}^{(1)} = \frac{2(2n+3)C_F}{(n+1)(n+2)} \left[\frac{(m+1)(m+2)}{(n-m)(n+m+3)} \left(2A_{nm} - \frac{\gamma_m^{(0)}}{2C_F} \right) + A_{nm} - S_1(n+1) \right], \quad (\text{A.16})$$

appear for $n > m$ and $n - m$ -even, where

$$A_{nm} = S_1((n+m+2)/2) - S_1((n-m-2)/2) + 2S_1(n-m-1) - S_1(n+1). \quad (\text{A.17})$$

-
- [1] A. P. Bakulev, S. V. Mikhailov and N. G. Stefanis, Phys. Lett. B **508**, 279 (2001) [Erratum-ibid. B **590**, 309 (2004)] [hep-ph/0103119].
- [2] A. P. Bakulev and S. V. Mikhailov, Phys. Rev. D **65**, 114511 (2002) [hep-ph/0203046].
- [3] V. M. Braun *et al.*, Phys. Rev. D **74**, 074501 (2006) [hep-lat/0606012].
- [4] A. Schmedding and O. I. Yakovlev, Phys. Rev. D **62**, 116002 (2000) [hep-ph/9905392].
- [5] A. P. Bakulev, S. V. Mikhailov and N. G. Stefanis, Phys. Rev. D **67**, 074012 (2003) [hep-ph/0212250].
- [6] V. L. Chernyak and A. R. Zhitnitsky, Nucl. Phys. B **201**, 492 (1982) [Erratum-ibid. B **214**, 547 (1983)].
- [7] T. Schafer and E. V. Shuryak, Phys. Rev. D **54**, 1099 (1996) [hep-ph/9512384].
- [8] V. Braun, P. Gornicki and L. Mankiewicz, Phys. Rev. D **51**, 6036 (1995) [hep-ph/9410318].
- [9] U. Aglietti, M. Ciuchini, G. Corbo, E. Franco, G. Martinelli and L. Silvestrini, Phys. Lett. B **441**, 371 (1998) [hep-ph/9806277].
- [10] A. Abada, P. Boucaud, G. Herdoiza, J. P. Leroy, J. Micheli, O. Pene and J. Rodriguez-Quintero, Nucl. Phys. Proc. Suppl. **106**, 338 (2002) [hep-lat/0110181].
- [11] J. Polchinski and M. J. Strassler, JHEP **0305**, 012 (2003) [hep-th/0209211].
- [12] S. J. Brodsky and G. F. de Teramond, Phys. Lett. B **582**, 211 (2004) [hep-th/0310227].
- [13] A. P. Bakulev, S. V. Mikhailov and N. G. Stefanis, Phys. Rev. D **73**, 056002 (2006) [hep-ph/0512119].
- [14] V. M. Braun, G. P. Korchemsky and D. Müller, Prog. in Part. and Nucl. Phys. **51**, 312 (2003) [hep-ph/0306057].
- [15] F. D. Aguila and M. Chase, Nucl. Phys. **B193**, 517 (1981).
- [16] E. Braaten, Phys. Rev. D **28**, 524 (1983).
- [17] E. Kadantseva, S. Mikhailov and A. Radyushkin, Sov. J. Nucl. Phys. **44**, 326 (1986).
- [18] F. M. Dittes and A. V. Radyushkin, Phys. Lett. B **134**, 359 (1984).
- [19] M. H. Sarmadi, Phys. Lett. B **143**, 471 (1984).
- [20] S. V. Mikhailov and A. V. Radyushkin, Nucl. Phys. B **254**, 89 (1985).
- [21] D. Müller, Phys. Rev. D **49**, 2525 (1994).
- [22] B. Melić, B. Nizić and K. Passek, Phys. Rev. D **65**, 053020 (2002) [hep-ph/0107295].
- [23] D. Müller, Phys. Rev. D **58**, 054005 (1998) [hep-ph/9704406].
- [24] A. Belitsky and D. Müller, Phys. Lett. B **417**, 129 (1997) [hep-ph/9709379].
- [25] M. Diehl, P. Kroll and C. Vogt, Eur. Phys. J. C **22**, 439 (2001) [hep-ph/0108220].
- [26] B. Melić, D. Müller and K. Passek-Kumerički, Phys. Rev. D **68**, 014013 (2003) [hep-ph/0212346].
- [27] E. B. Zijlstra and W. L. van Neerven, Nucl. Phys. B **383**, 525 (1992).
- [28] S. Larin and J. Vermaseren, Phys. Lett. B **259**, 345 (1991).
- [29] D. Müller, Phys. Rev. D **51**, 3855 (1995) [hep-ph/9411338]; *ibid.* **59**, 116003 (1999) [hep-ph/9812490].
- [30] P. Ball, V. M. Braun and A. Lenz, JHEP **05**, 004

- (2006) [hep-ph/0603063].
- [31] V. Braun and I. Filyanov, *Z. Phys. C* **48**, 239 (1990).
 - [32] S. Bethke, *J. Phys. G* **26**, R27 (2000) [hep-ex/0004021].
 - [33] K. G. Chetyrkin, J. H. Kuhn and M. Steinhauser, *Comput. Phys. Commun.* **133**, 43 (2000) [hep-ph/0004189].
 - [34] E. Floratos, D. Ross and C. Sachrajda, *Nucl. Phys. B* **129**, 66 (1977), [Erratum-ibid. B **139**, 545 (1978)].
 - [35] A. Retey and J. Vermaseren, *Nucl. Phys. B* **604**, 281 (2001) [hep-ph/0007294].
 - [36] E. Zijlstra and W. van Neerven, *Nucl. Phys. B* **417**, 61 (1994) [Erratum-ibid. B **426**, 245 (1994), B **773**, 105 (2007)].
 - [37] V. M. Braun, E. Gardi and S. Gottwald, *Nucl. Phys. B* **685**, 171 (2004) [hep-ph/0401158].
 - [38] S. Descotes-Genon and C. T. Sachrajda, *Nucl. Phys. B* **650**, 356 (2003) [hep-ph/0209216].
 - [39] S. W. Bosch, R. J. Hill, B. O. Lange and M. Neubert, *Phys. Rev. D* **67**, 094014 (2003) [hep-ph/0301123].
 - [40] M. Beneke and T. Feldmann, *Nucl. Phys. B* **685**, 249 (2004) [hep-ph/0311335].
 - [41] V. M. Braun, D. Y. Ivanov and G. P. Korchemsky, *Phys. Rev. D* **69**, 034014 (2004) [hep-ph/0309330].
 - [42] S. J. Lee and M. Neubert, *Phys. Rev. D* **72**, 094028 (2005) [hep-ph/0509350].
 - [43] V. L. Chernyak and A. R. Zhitnitsky, *Phys. Rept.* **112**, 173 (1984).
 - [44] V. Braun, R. J. Fries, N. Mahnke and E. Stein, *Nucl. Phys. B* **589**, 381 (2000) [Erratum-ibid. B **607**, 433 (2001)] [hep-ph/0007279].